The Astrophysical Journal, 576:587–598, 2002 September 1

ON THE PHENOMENOLOGY OF HYDRODYNAMIC SHEAR TURBULENCE

Pierre-Yves Longaretti
Laboratoire d'Astrophysique de Grenoble, BP 53X, Grenoble Cedex 9, 38410, France; Pierre-Yves.Longaretti@obs.ujf-grenoble.fr
Received 2002 March 25; accepted 2002 May 8

ABSTRACT

The question of a purely hydrodynamic origin of turbulence in accretion disks is reexamined, on the basis of a large body of experimental and numerical evidence on various subcritical (i.e., linearly stable) hydrodynamic flows. One of the main points of this paper is that the length scale and velocity fluctuation amplitude that are characteristic of turbulent transport in these flows scale as $\mathrm{Re}_m^{-1/2}$, where Re_m is the minimal Reynolds number for the onset of fully developed turbulence. From this scaling, a simple explanation of the dependence of Re_m with relative gap width in subcritical Couette-Taylor flows is developed. It is also argued that flows in the shearing sheet limit should be turbulent, and that the lack of turbulence in all such simulations performed to date is most likely due to a lack of resolution, as a consequence of the effect of the Coriolis force on the large-scale fluctuations of turbulent flows. These results imply that accretion flows should be turbulent through hydrodynamic processes. If this is the case, the Shakura-Sunyaev α parameter is constrained to lie in the range 10^{-3} to 10^{-1} in accretion disks, depending on unknown features of the mechanism that sustains turbulence. Whether the hydrodynamic source of turbulence is more efficient than the MHD one where present is an open question.

Subject headings: accretion, accretion disks — hydrodynamics — turbulence

1. INTRODUCTION

The need for turbulent transport to account for the rather short accretion/ejection timescales of young stellar objects (YSOs) and binary systems (cataclysmic variables, X-ray binaries), or for the very large energy output of active galactic nuclei (AGNs), is a well-known feature of accretion disk theory. From the very beginning, differential rotation has been regarded as one of the most promising sources for turbulence, since shear flows are known to be able to feed both hydrodynamic and MHD instabilities.

In most accretion disk models, the angular velocity profile satisfies Rayleigh's criterion, implying that the corresponding hydrodynamic flow is linearly stable. This is the case in particular of the nearly Keplerian velocity profile of cold disk models. However, finite-amplitude instabilities are theoretically known to occur in some linearly stable flows, and are believed to cause the turbulence observed in actual experiments, e.g., in planar Couette flows, or Couette-Taylor flows with the inner cylinder at rest. Furthermore, shear-driven hydrodynamic turbulence would certainly produce the required outward transport of angular momentum for Keplerian flows, because of their outwardly decreasing angular velocity profile. For these reasons, turbulence in accretion disks (magnetized or not) has long been widely believed to originate in purely hydrodynamic phenomena.

This picture has been seriously challenged in the past decade. First, Balbus & Hawley (1991) have shown that a local version of the magnetorotational instability (Chandrasekhar 1960) operates in differentially rotating disk. This instability was later recognized to give rise to MHD turbulence and transport as well as to magnetic field amplification (Hawley, Gammie, & Balbus 1995; Brandenburg et al. 1995). The physics of the magnetorotational instability is by now a well-established aspect of accretion disk theory. Second, recent simulations of hydrodynamic fluid flows in the shearing sheet approximation strongly suggest that accretion disk flows cannot become turbulent through hydrodynamic processes alone (Balbus, Hawley, & Stone 1996; Hawley, Balbus, & Winters 1999); indeed, in these simulations, planar Couette flows are observed to be turbulent, but turbulence disappears as soon as a Coriolis force is added, suggesting that this force prevents the onset of the finite-amplitude instabilities through which linearly stable flows are believed to become turbulent. Although this last finding seems to conflict with the available experimental evidence on Couette-Taylor flows (Richard & Zahn 1999), it has strengthened the idea that linear magnetic instabilities play a key role in the onset of turbulence in accretion disks.

The main objective of this paper is to critically reinvestigate the possibility of hydrodynamic turbulent motions in accretion disks, especially for linearly stable flows. A possible hydrodynamic origin of turbulent motions is important for several reasons. First, differential rotation is universally present in disks, whereas some disks or disk regions might not be ionized enough to support MHD phenomena, and a non-MHD source of turbulence must be at work there. For instance, protoplanetary disks are probably too resistive to support MHD turbulence (Fleming, Stone, & Hawley 2000; Sano et al. 2000), but their observationally constrained accretion rates imply the existence of turbulent transport. Second, the existence of self-consistent magnetized accretion/ejection structures seems to require a quasi equipartition of thermal and magnetic energy which, combined with the vertical stratification of these structures, may prevent the development of the magnetorotational instability in a number of instances (Ferreira 1997; Casse & Ferreira 2000).

The objectives of this paper are achieved through two different means. First, relevant pieces of information on the behavior of various types of shear flows that are available in the specialized fluid dynamical literature are presented; from this material, it is argued that shearing sheet flows should be turbulent. Second, a phenomenological description and understanding of relevant turbulent properties of

shear flows as they appear in the available experiments and numerical simulations is developed. In its most basic form, the phenomenology of hydrodynamic turbulent flows often relies on the concepts of Kolmogorov cascade and turbulent viscosity, and this approach is adopted here. Although the turbulent viscosity concept is of limited validity in complex situations (Tennekes & Lumley 1972) and its use in the assessment of stability properties of turbulent flows has been rightly criticized (see, e.g., Terquem 2001; Hawley, Balbus, & Stone 2001), it is well known to provide accurate scalings of mean flow properties in simple shear flows such as channel or planar Couette flows (Tennekes & Lumley 1972; Lesieur 1987); consequently, it has been widely used to parameterize turbulent transport in accretion disks. In this paper, some new and interesting consequences of this *Ansatz* and their implications for turbulence in shear flows are pointed out.

This paper is organized as follows. In the next section, some relevant flow configurations are introduced, along with the related forms of the Navier-Stokes equations; I also summarize relevant features of turbulence in these flows, as found in the literature, since this material has some direct bearing on the question of hydrodynamic turbulence in accretion disks, and is largely unknown to the astrophysical community; the reader who is not interested in factual details but only in their significance can jump directly to § 2.4, where this material is used to infer that "perfect" shearing sheet simulations should be turbulent. The most interesting findings of the present work are collected in § 3; after briefly recalling the origin and rationale of the turbulent viscosity prescription, some of its previously unnoticed but important consequences are derived and used to interpret the behavior of the flows previously described, with special attention paid to Couette-Taylor flows, and to flow description in the shearing sheet approximation.In particular, a phenomenological explanation of the scaling of the Reynolds number with gap width in subcritical Couette-Taylor flows is devised. On the basis of this phenomenological understanding, the various reasons that might likely prevent the onset of turbulence in the simulations of Balbus et al. (1996) and Hawley et al. (1999) are discussed and the most critical one identified. The final section summarizes the most relevant conclusions and discusses their consequences for accretion disk theory and simulation, in particular on the magnitude of the Shakura-Sunyaev α parameter.

The reader interested only in the new results of this paper and not in the background fluid mechanical information can focus on §§ 2.4, 3.2–3.4, and 4.

2. TURBULENCE IN HYDRODYNAMIC SHEAR FLOWS

Hydrodynamic accretion disk mean flows are widely believed to be subcritical, i.e., the viscously relaxed laminar flow is linearly stable at all Reynolds numbers, at least locally. Furthermore, all experiments and numerical simulations of interest here pertain to linearly stable flows, and we are mostly interested in the local generation of turbulence. Therefore, I focus on subcritical flows in this paper.

The transition to turbulence is usually rather different in subcritical and supercritical flows. Supercritical flows undergo a cascade of precisely defined bifurcations in parameter space, eventually leading to fully developed turbulence; these transitions are well documented and reproduced numerically, e.g., for Couette-Taylor flows (Andereck, Liu, & Swinney 1986 and references therein; Marcus 1984a, 1984b). Turbulence in subcritical flows, on the contrary, may be abruptly triggered, most probably by finite-amplitude instabilities (Dauchot & Daviaud 1994); also, the flow apparently evolves from highly intermittent to fully turbulent over a range of Reynolds numbers.

Furthermore, shear flows can be either (wall-)bounded or free. The distinction refers to the limitation of the flow in the direction in which the shear is applied (the transverse or shearwise direction). This difference in boundary conditions influences some of their turbulent properties; indeed, free flows are characterized by a single length scale, the extent of the shear layer, whereas the distance to the wall introduces a second length scale in wall-bounded flows. The influence of the other (streamwise and spanwise) boundaries is minimized inasmuch as their spacing exceeds the coherence length of the largest turbulent eddies, and as globally induced perturbations (such as Ekman circulation) are minimized by appropriate designs of the experimental setups.

Shear flows have been actively studied in the past decades, and their turbulent properties are now characterized for a large variety of settings. In this section, I briefly present the subcritical flows that have direct bearing on the question of hydrodynamic turbulence in accretion disks, namely, plane Couette and free shear flows, either rotating or not; Couette-Taylor flows; and Rayleigh-stable tidally driven shear flows in the shearing sheet approximation. The first two have been studied through both experiments and numerical simulations. However,information on Rayleigh stable Taylor-Couette flows comes only from experiments. Finally, the shearing sheet approximation has been widely used as a local analytic model of local accretion disks, and has been implemented in the numerical work of Balbus, Hawley, and coworkers quoted in the introduction (Balbus et al. 1996; Hawley et al. 1999). For each of these flows, I characterize the geometry and the critical parameters that are important for the question of the onset of turbulence, and I also give the governing dynamical equation (Navier-Stokes) in the form most suitable to establishing comparisons between the various types of flows.

The object of this section is to try to give an answer to the following question: If numerical simulations were perfect (i.e., not limited by questions of resolution, numerical instabilities, etc.), would shear flows be turbulent in the presence of the Coriolis force? This is done in § 2.4, with the help of the material collected here.

2.1. *Plane Couette and Free Shear Flows*

In spite of their conceptual simplicity, plane Couette flows are difficult to produce in actual experiments, which explains why some of their basic turbulent properties have only recently been characterized. The experimental setup is schematically represented in Figure 1, along with a sketch of the turbulent mean flow profile (see Tillmark & Alfredsson 1992 for details). In practice, the two walls are often made up of countermoving (looped) infinite belts. Similarly, free shear layers are produced by injecting fluid with different velocities on each side of a separating plate. The fluids come in contact at the end of the plate, and a turbulent layer develops and widens downstream (see Fig. 2).

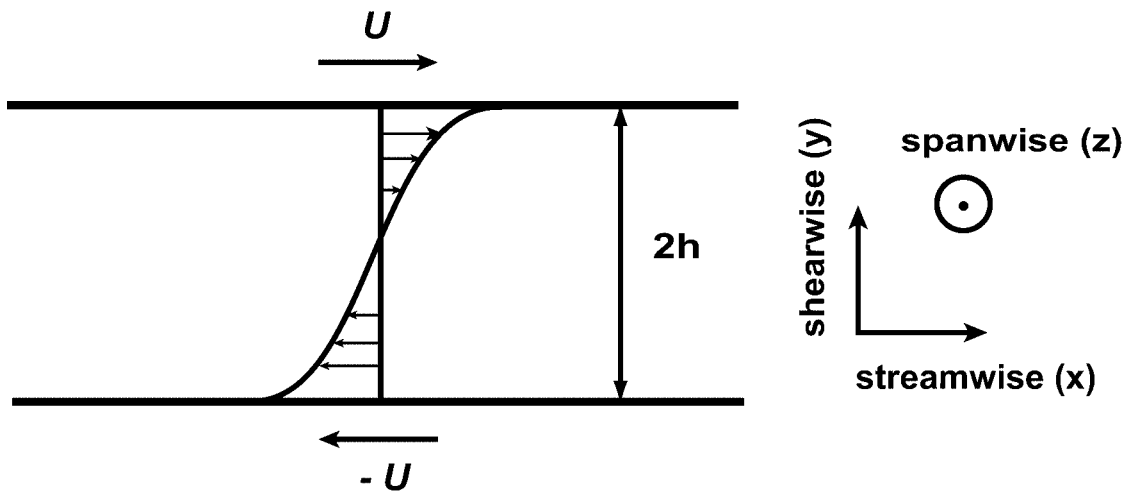

FIG. 1.—Sketch of the configuration of Couette flows. The flow is bounded by two countermoving walls, and boundary layers develop in the turbulent regime, as shown by the mean velocity profile. By putting the experimental setup on a rotating platform, one obtains the so-called rotating Couette flow.

These flows are described by the Navier-Stokes equation in its simplest form, which reads

$$\frac{\partial \boldsymbol{v}}{\partial t} + \boldsymbol{v} \cdot \boldsymbol{\nabla} \boldsymbol{v} = -\frac{\boldsymbol{\nabla} P}{\rho} + \nu \Delta \boldsymbol{v} \,, \tag{1}$$

with obvious notations. The viscous terms are displayed in the incompressible form, since we are mostly concerned with subsonic turbulence.

It is customary to define the Reynolds number of plane Couette flows based on the half-velocity difference (i.e., U) and half-width distance (i.e., h) between the two walls. However, for the purpose of comparison with other setups, I define the Reynolds number as

$$\mathrm{Re} = 4Uh/\nu \,, \tag{2}$$

i.e., based on the total velocity difference and distance between the two boundaries; the reader should bear in mind the resulting factor of 4 when comparing the figures quoted in this paper for Couette flows with the literature. From the experiments of Tillmark & Alfredsson (1992), the minimal Reynolds for which turbulence is sustained is $\mathrm{Re} \simeq 1500$. The onset of turbulence in planar Couette flow has been successfully reproduced in numerical simulations (e.g., Bech et al. 1995 and references therein); a nonlinear mechanism for tapping the mean shear to sustain turbulence has even been identified (e.g., Jiménez & Moin 1991; Hamilton, Kim, & Waleffe 1995; Waleffe 1997).

Rotating Couette and rotating free shear flows are produced by placing the experimental setup on a rotating platform. Such flows are very relevant to astrophysics, since they share a number of features with accretion disk flows in the shearing sheet approximation. For these flows, the Navier-Stokes equation reads

$$\frac{\partial \boldsymbol{v}}{\partial t} + \boldsymbol{v} \cdot \boldsymbol{\nabla} \boldsymbol{v} = -\frac{\boldsymbol{\nabla} P}{\rho} - 2\boldsymbol{\Omega} \times \boldsymbol{v} + \boldsymbol{F}_{\mathrm{in}} + \nu \Delta \boldsymbol{v} \,, \tag{3}$$

where $\boldsymbol{F}_{\mathrm{in}}$ stands for the inertial force due to rotation.

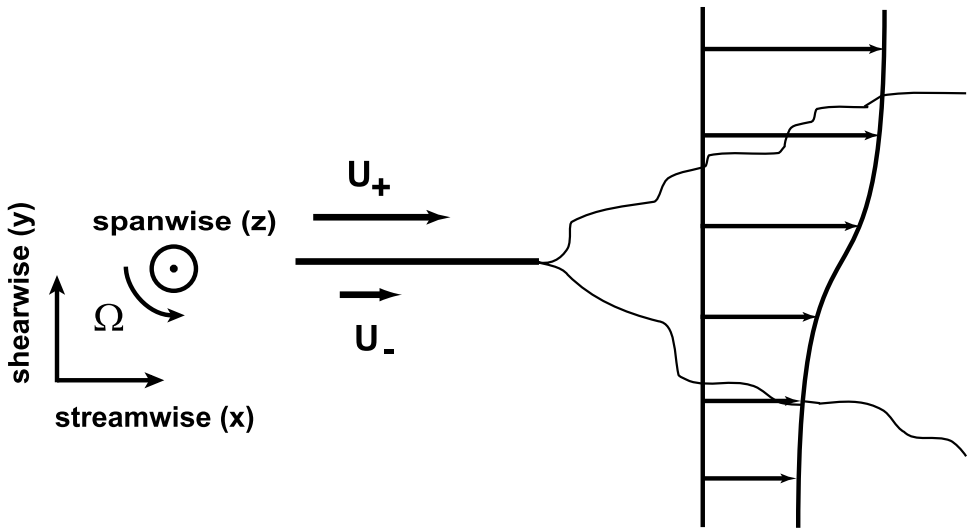

FIG. 2.—Sketch of the configuration of (rotating) free shear layers. Two layers of fluid of different velocities, initially horizontally separated, come in contact at the end of a dividing plate, and a turbulent shear layer develops and widens downstream.

These rotating flows are usually simulated by including only the Coriolis force term[1] in the Navier-Stokes equation (Bech & Andersson 1996a, 1997; Komminaho, Lundbladh, & Johansson 1996), so that equation (3) reduces to

$$\frac{\partial \boldsymbol{v}}{\partial t} + \boldsymbol{v} \cdot \boldsymbol{\nabla} \boldsymbol{v} = -\frac{\boldsymbol{\nabla} P}{\rho} - 2\boldsymbol{\Omega} \times \boldsymbol{v} + \nu \Delta \boldsymbol{v} \, . \tag{4}$$

Rotating Couette and rotating free shear flows are characterized by the ratio S of the angular velocity of rotation to the shear,

$$S = -\frac{2\Omega}{d\langle v_x \rangle / dy} \, , \tag{5}$$

where $\langle v_x \rangle$ is the mean velocity profile; this number is akin to an inverse Rossby number, and measures the relative strength of the Coriolis and advection terms in the Navier-Stokes equation. A linear shear is destabilized by rotation when

$$-1 < S < 0 \, , \tag{6}$$

and stabilized otherwise (see Tritton 1992 and references therein; see also § 2.4). The relevant regime for astrophysics is $S \lesssim -1$ (i.e., negative S and linearly stable linear shear[2]). No systematic exploration of the (Re, S) parameter space has been performed; furthermore, I am not aware of any experimental investigation of rotating Couette flows for such (relatively) high values of S. However, this regime is explored in the set of free shear layer experiments of Bidokhti & Tritton (1992), who show that the flow remains turbulent[3] (although linearly stable) down to $S \sim -2$ for Reynolds numbers[4] $\sim$4000 (see Figs. 14 and 16 of their paper). On the other hand, in the numerical simulations of anticyclonic ($S < 0$) rotating Couette flows of Bech & Andersson (1997) (Re $\sim$ 5000) and Komminaho et al. (1996) (Re $\sim$ 3000), turbulence is lost[5] for $S \sim -1$ in the central part of the flow. This situation is similar to the one relating the simulations of Balbus et al. (1996) and Hawley et al. (1999) to the experimental data of Taylor (1936) and Wendt (1933) quoted in Richard & Zahn (1999); this analogy will be further discussed in §§ 2.4 and 3.4.

[1] The centrifugal term is not included on the basis that it results only in a redistribution of the equilibrium pressure.

[2] In relating rotating flows to shearing sheet ones, note that the y-axis identifies to the radial one, whereas the x and azimuthal directions are antiparallel.

[3] By virtue of the Taylor-Proudman theorem, the flow should eventually become bidimensional, but this happens only at higher values of $|S|$.

[4] Note that, as the turbulent shear layer widens downstream, Bidokhti & Tritton (1992) base their definition of the Reynolds number on the downstream distance x, which needs to be related to the layer width from which all Reynolds numbers quoted here are defined, and which is referred to as $2\delta_M$ in their paper. The two quantities can be related with the help of the various relations given in § 3 of their paper. This amounts to reducing the Reynolds numbers they quote by a factor of $\sim$7. Finally, the number given above corresponds to the most downstream point of measurement, where the flow should be closest to a developed (rather than developing) turbulent flow (incidentally, this is much farther downstream than the region where the pictures shown in the paper are taken).

[5] Rotation in these numerical experiments is characterized by a global rotation number $\mathrm{Rot} \equiv 2\Omega h / U$ rather than by the local rotation parameter S. In the central part of the profile, one usually has $\mathrm{Rot} \gtrsim 0.2|S|$ for fully turbulent flows, but it is difficult to precisely relate the relative level of rotation in these experiments to the critical limit between linearly stable and unstable rotating flows.

2.2. *Couette-Taylor Flows*

Couette-Taylor flows are produced from two concentric rotating cylinders. Most investigations of this type have focused on the linearly unstable regime. The linearly stable one, which is more directly relevant to astrophysics, has only been explored by Taylor (1936), who maintained the inner cylinder at rest, and by Wendt (1933), who also reported results when the flow is close to marginal stability (i.e., linearly stable, but close to constant specific angular momentum). The Reynolds number of these flows is defined as

$$\mathrm{Re} = \frac{r \Delta\Omega \Delta r}{\nu} \, , \tag{7}$$

where r is the mean of the two cylinder radii, and $\Delta\Omega$ and Δr are respectively the difference in angular velocity and the gap width of the two cylinders. Both investigations mentioned above did characterize the behavior of the minimal Reynolds number for well-developed turbulence to be maintained as a function of the cylinders' relative gap width; this behavior is sketched in Figure 3. Recently, a French team has undertaken an experimental investigation of flow profiles that are approximately Keplerian in the mean, and found that turbulence was also maintained for Reynolds numbers of the order of a few thousand for a relative gap width of the order of $\frac{1}{3}$ (Richard 2001).

The minimal Reynolds number appearing in Figure 3 is obtained by starting from an initially laminar flow, and progressively increasing the difference in angular velocity of the two cylinders (or only the outer cylinder angular velocity if the inner one is at rest). When starting from an initially turbulent flow and reversing the process, the loss of turbulence occurs for Reynolds numbers that can be significantly lower, but the flow is then highly intermittent; it is reasonable to assume that the minimal Reynolds numbers of

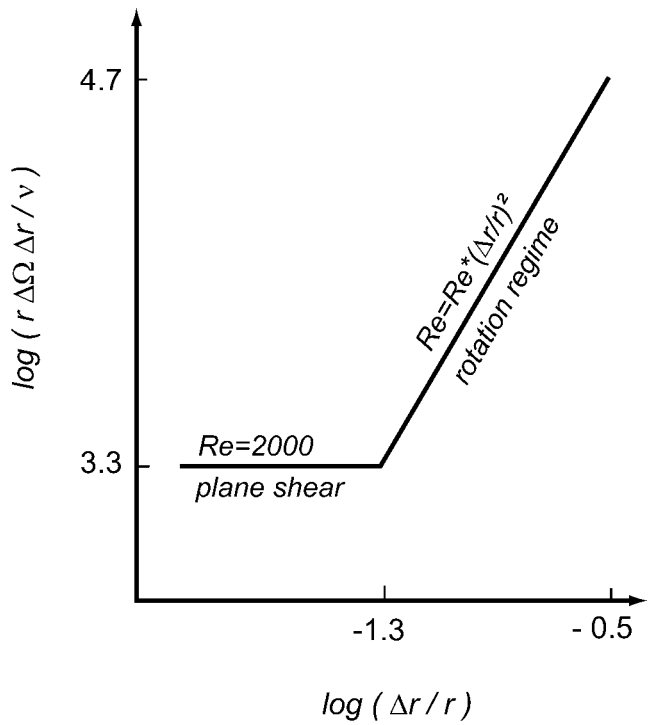

FIG. 3.—Idealized behavior of the minimal Reynolds number of fully turbulent Couette-Taylor flows, as a function of the relative gap width.

Figure 3 are characteristic, albeit overestimated, values for well-developed turbulence (Richard 2001).

The two remarkable features of this minimal Reynolds number are a behavior that is similar to plane Couette flows for $\Delta r/r \lesssim 1/20$, with $\mathrm{Re} \simeq 2000$, and a quadratic scaling [$\mathrm{Re} \simeq \mathrm{Re}^*(\Delta r/r)^2$ with $\mathrm{Re}^* \simeq 6 \times 10^5$] that is characteristic of rotation, as argued by Richard & Zahn (1999); these authors also show that in the same regime, the turbulent viscosity $\nu_t \simeq \beta r^3 |d\Omega/dr|$, with $\beta \simeq 10^{-5}$. A heuristic explanation of these features is presented in § 3.

The Navier-Stokes equation for these flows is most meaningfully compared to that of other flows when subtracting out the mean flow rotation Ω_0 (i.e., the average angular velocity of the two cylinders), since only differential rotation plays a role in the generation of turbulence. Defining $\boldsymbol{w} = \boldsymbol{v} - \Omega_0 r \boldsymbol{e}_\phi$, and $\phi = \theta - \Omega_0 t$ (so that $\boldsymbol{w}$ and ϕ are the velocity and azimuthal coordinate in the rotating frame, respectively), the Navier-Stokes equation for $\boldsymbol{w} = (w_r,\ w_\phi,\ w_z)$ becomes

$$\frac{\partial \boldsymbol{w}}{\partial t} + \boldsymbol{w} \cdot \boldsymbol{\nabla}' \boldsymbol{w} + 2\boldsymbol{\Omega} \times \boldsymbol{w} - \frac{w_\phi^2}{r}\boldsymbol{e}_r + \frac{2 w_\phi w_r}{r}\boldsymbol{e}_\phi = \left(-\frac{\boldsymbol{\nabla} P}{\rho} + r\Omega^2 \boldsymbol{e}_r \right) + \nu \Delta \boldsymbol{w} , \quad (8)$$

where

$$\boldsymbol{w} \cdot \boldsymbol{\nabla}' \boldsymbol{w} \equiv (\boldsymbol{w} \cdot \boldsymbol{\nabla} w_r)\boldsymbol{e}_r + (\boldsymbol{w} \cdot \boldsymbol{\nabla} w_\phi)\boldsymbol{e}_\phi + (\boldsymbol{w} \cdot \boldsymbol{\nabla} w_z)\boldsymbol{e}_z .$$

For future reference, I refer to the terms w_θ^2/r and $2 w_r w_\theta / r$ as "geometric terms," since they arise because of the cylindrical geometry.[6]

For these flows, the rotation parameter defined in equation (5) reads

$$S = \frac{2\Omega}{r d\Omega/dr} = -\frac{2}{q} , \quad (9)$$

where $q \equiv -(r/\Omega)(d\Omega/dr)$ is the parameter defined by Balbus et al. (1996) to characterize rotation profiles. The flow is stable according to Rayleigh's criterion when $q < 2$ (for $\Omega > 0$), i.e., when $S^{-1} > -1$, quite similarly to rotating Couette and free flows, although the processes through which instability occurs are different. Note also that equations (4) and (8) differ only through the geometric and centrifugal terms.

The fact that the minimum Reynolds number for developed turbulence is identical in plane Couette and Couette-Taylor flows with $\Delta r/r \lesssim 1/20$ and the inner cylinder at rest can be understood in the following way. First, the advection term (which is the source of the turbulence cascade, as indicated by the very existence of the Reynolds number) dominates over the geometric terms when $r\Delta\Omega/\Delta r \gg r\Delta\Omega/r$, i.e., $\Delta r/r \ll 1$. Second, $\Delta\Omega = \Omega$ (one cylinder being at rest), so that the Coriolis term is also very small compared to the advection term, and equation (8) nearly reduces to equation (1). Note furthermore that the Coriolis force does not appear to significantly affect the minimal Reynolds number for the onset of turbulence for the values of q of interest here (i.e., $q = -1$ to $q \sim 1$–2), both in the limiting plane Couette regime and in the rotation regime, as exemplified by the data of Wendt (1933) for nearly neutral flows, which follow the same law for the minimal Reynolds number, down to the plane Couette limit.

[6] Such terms also arise in principle from the viscous term, but they are inessential to the argument developed in this paper.

2.3. *Shearing Sheet*

Accretion disk flows in the shearing sheet approximation are closely related to the Couette-Taylor flows previously described. They differ in only three respects.

First, the mean angular velocity profile $\langle\Omega\rangle$ in Couette-Taylor flows is imposed by the boundary conditions, and by the condition of stationarity of the mean viscous or turbulent transport of angular momentum, from the azimuthal momentum equation (with the walls acting as source and sink of angular momentum). The radial momentum equation then imposes the mean radial pressure profile $\langle P\rangle$, and the resulting tidal force term $(-\nabla\langle P\rangle/\langle\rho\rangle + r\langle\Omega\rangle^2)$. On the contrary, in accretion disks, the mean radial angular velocity profile mostly results from the gravitational attraction of the central body, which imposes a nearly Keplerian profile in cold disks, but the disk is never globally stationary, because of viscous/turbulent transport (nevertheless, an approximate stationarity is nearly achieved locally on the dynamical timescales of interest for the onset of turbulence). Therefore, in Keplerian disks in the shearing sheet approximation, the tidal force term $(-g + r\langle\Omega\rangle^2)$ is the source of the (Keplerian) angular velocity profile and not its consequence. Furthermore, one usually neglects the radial pressure gradient locally, and assumes that the gravitational force has cylindrical (and not spherical) symmetry for simplicity, since cold disks are thin.

Second, a local approximation is performed, by restricting consideration to a radial box of width $\Delta r \ll r$; one also usually assumes that the height of the box is comparable to its width. Under these assumptions, one neglects the geometric terms in equation (8), and describes the flow in local Cartesian coordinates ($x \leftrightarrow r$, $y \leftrightarrow r\phi$, where ϕ is the azimuthal coordinate in the rotating frame introduced for Couette-Taylor flows). One also linearizes the angular velocity profile.

Finally, this local approximation and the resulting change of geometry from cylindrical to Cartesian (except for the Coriolis force term, which is kept) allows one, in numerical simulations, to adopt a particular form of the periodic boundary condition in the radial direction, in which the fluid quantities on the radial boundaries are longitudinally displaced all the time with the mean angular velocity difference during a time step before the periodic boundary condition is applied (see Hawley et al. 1995 for details on this procedure).

With these prescriptions (aside from the boundary conditions), the Navier-Stokes equation, in the shearing sheet approximation and in the rotating frame, becomes

$$\frac{\partial \boldsymbol{w}}{\partial t} + \boldsymbol{w} \cdot \boldsymbol{\nabla} \boldsymbol{w} + 2\boldsymbol{\Omega} \times \boldsymbol{w} = -\frac{\boldsymbol{\nabla} P}{\rho} + 2q\Omega^2 x \boldsymbol{e}_r + \nu \Delta \boldsymbol{w} , \quad (10)$$

where $x = r - r_0$, and r_0 is the position of the center of the shearing sheet box. The term $2q\Omega^2 x$ represents the tidal force (difference of the gravitational and inertial force); q is the parameter introduced in § 2.2 and measures the steepness of the rotation profile. Note that the pressure term contains only fluctuations related to the presence of turbulence, which is not the case in Couette-Taylor flows. It is interesting to note that this equation shares features with both equations (4) and (8); in particular, linear stability is ensured for $q < 2$, i.e., $S < -1$ for the laminar linear profile. This makes the loss of turbulence in the simulations of Balbus et

al. (1996) and Hawley et al. (1999), for values of q smaller than 2 by a few percents only, all the more intriguing.

2.4. *Shearing Sheet, Rotating Couette Flows, and Turbulence*

In fact, all available pieces of evidence strongly suggest that numerical simulations of rotating Couette flows and of tidally driven sheared motions in the shearing sheet limit should display turbulence, as I argue now.

First, plane Couette flows, rotating Couette flows, and tidally driven shearing sheet flows have similar linear stability properties. For all three types of flows, the viscously relaxed laminar solution is a simple linear shear, which is always linearly stable for the plane Couette flow,[7] and stable for the other two flows once $S < -1$ (which is the only case of interest here). Plane Couette flows are subject to finite-amplitude instabilities (see, e.g., Lerner & Knobloch 1998; Dubrulle & Zahn 1991; and references therein). The same is true of rotating Couette flows (Johnson 1963), and of shearing sheet flows (Dubrulle 1993). As finite-amplitude instabilities are considered to trigger the turbulence seen both in experimental and numerical investigations of plane Couette flow, one would expect the same to be true of the other two flows.

Second, let us reexamine the differences between rotating Couette flows and the shearing sheet flows with the other flows discussed previously. They amount to differences of boundary conditions, of mean force terms, and of geometry.

The shearing sheet boundary conditions are in a way intermediate between rigid and free boundary conditions, since they imply that the mean flow obeys rigid boundary conditions, whereas the fluctuating part obeys periodic boundary conditions; rotating Couette flow simulations are usually performed with rigid boundary conditions. On the one hand, Couette-Taylor flows implement rigid boundary conditions. Although in real experiments the vibrations of the boundary play some role in triggering turbulent motions, there is little doubt that in these experiments, turbulence is self-sustained. On the other hand, from the experiments of Bidokhti & Tritton (1992), the rotating shear flows with free boundary conditions are turbulent, although by construction no mean steady state can be reached in these systems. Therefore, it seems unlikely that boundary conditions play an important role in the presence or absence of turbulence in numerical experiments.

In the shearing sheet approximation, the mean shear is imposed by the tidal force term; in rotating Couette simulations, it results from the boundary conditions. In Couette-Taylor flows, the boundary conditions not only produce the shear, but also generate a mean radial pressure gradient. Note, however, that the term $-d\langle P\rangle/dr/\langle\rho\rangle + r\langle\Omega\rangle^2$ of equation (8) is similar in function to the term $2q\Omega^2 x$ in equation (10). Furthermore, the mean pressure gradient in Couette-Taylor experiments is radial, whereas it is longitudinal (streamwise) in the rotating free shear layer experiments of Bidokhti & Tritton (1992). This suggests that neither large-scale mean pressure gradients nor tidal terms make any significant difference to the question of the onset of turbulence in the various flows considered here, especially since all gradient terms get out of the way in incompressible flows (they disappear from the vorticity equation).

Finally, I show in the next section that the main effect of the geometry (which enters through the geometric terms in Couette-Taylor flows) is to change the conditions of onset of turbulence, but this does not affect the occurrence of turbulence in itself.

Although such arguments do not exclude more complex possibilities (e.g., that turbulence might be impeded in shearing sheet flows by a combination of these factors instead of only one of them), this strongly indicates that rotating Couette flows and shearing sheet ones should be turbulent, suggesting that the absence of turbulence in all the published simulations of this kind stems from limitations in the numerics involved. This last point is addressed in the next section.

3. PHENOMENOLOGY OF SUBCRITICAL TURBULENCE

The purpose of this section is to point out important features of turbulence in sheared flows, through a phenomenological model developed in § 3.2. The consequences of this model are used in § 3.4 to identify the potential limitations of the numerics just mentioned.

3.1. *Turbulent Viscosity and the Kolmogorov Prescription*

In a picture in which the fluctuating turbulent scales can be separated from the more regular large ones, it is meaningful to write down an equation for both the mean $\langle X\rangle$ and fluctuating δX parts of any quantity X. In particular, the evolution of the mean velocity reads

$$\frac{\partial\langle\boldsymbol{v}\rangle}{\partial t} + \boldsymbol{\nabla}\cdot\langle\overline{\overline{\delta\boldsymbol{v}\delta\boldsymbol{v}}}\rangle = -\frac{\boldsymbol{\nabla}\langle P\rangle}{\rho} + \nu\Delta\langle\boldsymbol{v}\rangle\ , \tag{11}$$

where possible geometric and/or inertial terms, as well as the effect of compressibility, have been omitted for simplicity. In the simple shear configurations of interest here, only the $\langle\delta v_y\delta v_x\rangle$ (or $\langle\delta v_r\delta v_\phi\rangle$) part of the Reynolds stress tensor is relevant for radial turbulent transport.

By describing turbulent fluctuations with a characteristic coherence scale l_M and velocity amplitude v_M, Prandtl (1925) argued that

$$\langle\delta v_y\delta v_x\rangle \sim v_M^2 \sim \nu_t\frac{d\langle v_x\rangle}{dy}\ , \tag{12}$$

with

$$\nu_t \sim l_M v_M\ . \tag{13}$$

Note that in cylindrical geometry, $\langle\delta v_r\delta v_\phi\rangle \sim \nu_t r d\langle\Omega\rangle/dr$.

The reasoning behind this formulation is similar to the reasoning relating the usual molecular viscosity to the molecular mean free path and velocity dispersion (i.e., turbulent transport occurs over a "mean free path" l_M with "velocity dispersion" v_M); equation (12) can also be derived from more rigorous multiscale expansion techniques. In a Kolmogorov cascade picture, l_M is the energy-injection scale (and characterizes the coherence length of the largest eddies of the cascade), and v_M the amplitude of the velocity fluctuations at this scale, as the velocity amplitude decreases with decreasing scale in a Kolmogorov spectrum. However, this does not mean that larger fluctuating scales

[7] I consider unbounded flows in this discussion, since instabilities due to the boundary in viscous fluids are not relevant in astrophysics.

are not present in the flow, nor that they have no influence in the development of turbulence; it just implies that they dominate neither the energy spectrum nor the turbulent transport.

An important feature of the turbulent viscosity prescription is that the rate of energy dissipation ϵ (which is also the rate of energy transfer in eddy-scale [Fourier] space) is simply given by

$$\epsilon \sim v_M^3/l_M \sim \begin{cases} \nu_t(d\langle v_x\rangle/dy)^2 & \text{(Cartesian)}\,, \\ \nu_t(rd\langle\Omega\rangle/dr)^2 & \text{(cylindrical)}\,, \end{cases} \tag{14}$$

as can be shown most directly by deriving the relevant macroscopic energy equation. Equations (12) and (14) imply in particular that the characteristic frequency of turbulent motions is the shear frequency, i.e.,

$$\frac{v_M}{l_M} \sim \begin{cases} d\langle v_x\rangle/dy & \text{(Cartesian)}\,, \\ rd\langle\Omega\rangle/dr & \text{(cylindrical)}\,. \end{cases} \tag{15}$$

This reflects the fact that an externally imposed shear locally possesses no characteristic scale (besides the scale of the flow), but only a characteristic frequency, so that shear turbulence can only couple efficiently to the shear if its characteristic frequency or coherence time (at the energy-injection scale imposed by the mechanism that drives turbulence) matches the shear frequency.[8]

The turbulent viscosity description has been applied to a wide variety of setups to describe the mean properties of turbulent flows, both in the vicinity of walls and in the main part of either free or bounded flows (e.g., Tennekes & Lumley 1972; Lesieur 1987).

3.2. *Turbulence Scales: Phenomenological Model and Orders of Magnitude*

My primary purpose here is to point out some interesting consequences of the turbulent viscosity prescription. Indeed, one expects that a flow undergoes a transition to turbulence when the turbulent transport becomes more efficient than the laminar one for subcritical flows. This implies that

$$\nu_t \gtrsim \nu \qquad \text{when } \mathrm{Re} \gtrsim \mathrm{Re}_m\,, \tag{16}$$

where Re_m stands for the minimum Reynolds numbers for the onset of turbulence, discussed in § 2. For example, note that for Couette-Taylor flows, from the data of Wendt (1933) and Taylor (1936) $\nu_t/\nu \sim \beta\mathrm{Re}^* \sim 6$, where β and Re^* are the quantities introduced in the previous section in the discussion of these flows; furthermore, when the minimal Reynolds number is searched for by decreasing the velocity difference between the cylinder from an initially turbulent state instead of increasing it from an initially laminar one, the ratio ν_t/ν is sensibly closer to unity (Richard 2001).

Away from boundary layers (if any), the only scales that are relevant for characterizing the shear gradient are the typical size of the shear flow, Δy in Cartesian geometry (Δr in cylindrical geometry), and the typical shear amplitude over this scale, Δv_x ($r\Delta\Omega$ cylindrical). Combining equations (12), (14), and (16) then yields, for the bulk of the turbulent flow,

$$l_M \sim \begin{cases} \Delta y/\mathrm{Re}_m^{1/2} & \text{(Cartesian)}\,, \\ \Delta r/\mathrm{Re}_m^{1/2} & \text{(cylindrical)}\,, \end{cases} \tag{17}$$

and

$$v_M \sim \begin{cases} \Delta v_x/\mathrm{Re}_m^{1/2} & \text{(Cartesian)}\,, \\ r\Delta\Omega/\mathrm{Re}_m^{1/2} & \text{(cylindrical)}\,. \end{cases} \tag{18}$$

I wish to stress that equations (17) and (18) do not imply that turbulence is a global rather than local phenomenon. On the contrary, equations (14) and (15) relate l_M and v_M to local characteristics of the mean flow. Note that these relations justify (at least for subcritical flows) the separation of scales between the mean large-scale flow and the fluctuating small-scale one assumed in the turbulent viscosity description, because Re_m usually exceeds a few thousand.

These relations have a direct physical interpretation. Consider for example two planar Couette flows with identical shear rates, and with wall spacing Δy and relative velocity Δv_x, which differ by a given ratio. Obviously, the scaling with Δy and Δv_x is a natural consequence of the scaling similarity between flows that are otherwise *identical*. On the other hand, consider *different* flows, with identical shear rates, but different minimal Reynolds numbers (e.g., plane Couette and Couette-Taylor flows with appropriate parameters). A larger minimal Reynolds number is a sign of a greater difficulty in triggering turbulence, i.e., an increased difficulty for turbulent transport to dominate over the viscous one, and therefore is a sign of a smaller scale turbulence, as a result of the physical picture underlying the turbulent viscosity prescription (i.e., the transport occurs over a smaller "mean free path" l_M, and correspondingly with a smaller "random velocity" v_M, because of the assumption of identical shear rate between the two different flows).

From these relations, one can easily check that, at the minimum Reynolds number, the advection term, which dominates scale coupling and is the primary cause of the inertial turbulent spectrum, is comparable to the dissipation term, at the turbulent transport scale. As a consequence, the turbulence possesses little or no inertial domain at its threshold. Furthermore, as long as there is no change in the turbulence-generating process, increasing the Reynolds number can only result in lowering the dissipation scale with respect to l_M, and therefore in the progressive build-up of an inertial spectrum (e.g., imagine one does this by reducing the viscosity while maintaining the large-scale structure of the flow unchanged).

It is important to note that the estimates of equations (17) and (18) remain valid for Reynolds numbers larger than the turbulence threshold, as long as the turbulence-generating process is unchanged. The predictions of the scaling proposed here are well supported by the available empirical and numerical evidence, as shown in the Appendix.

3.3. *Consequences: Couette-Taylor Flows*

Equations (17) and (18) have particularly interesting consequences for the understanding of turbulence in Couette-Taylor flows. For definiteness, I first focus on flows in which the inner cylinder is at rest. As argued at the end of § 2.2, for

[8] As the coherence time of smaller scale eddies is shorter, they are less or little affected by the shear. As a consequence, in a first approximation, the turbulence is more or less isotropic at scales less than l_M, and anisotropy is ignored in the whole argument.

$r \gg \Delta r$, the Navier-Stokes equation for Couette-Taylor flows (eq. [8]) then reduces to the Navier-Stokes equation for planar Couette flows (eq. [1]), and the minimal Reynolds number is constant. However, when $\Delta r \to r$, the geometric terms $O(w^2/r) \sim (r\Delta\Omega)^2/r$ become comparable to the advection term on a scale Δr. Furthermore, if, at some radial location r in the flow, Re_m remained constant when $\Delta r \gg r$, equation (17) would imply that l_M could become arbitrarily larger than r, which makes little sense. In fact, one expects that $l_M \propto r$ once $\Delta r/r$ exceeds some critical ratio Δ_c (which for the time being is expected to be of order unity), for two reasons: first, the geometric terms introduce a limiting scale (the radius r), which must be accounted for by the turbulent viscosity description;[9] second, this prescription for l_M is necessary to satisfy the requirement that $w\nabla w \gtrsim w^2/r$ at the largest scale of the inertial spectrum (in order to maintain such a spectrum). Consequently, let us assume that

$$l_M \sim \gamma r \,, \tag{19}$$

where $\Delta r/r > \Delta_c$, and where γ is a constant to be determined later. The argument presented here suggests that $\Delta_c \sim 1$, whereas the data imply that it is significantly smaller than unity (see below); as for the large values of the minimal Reynolds numbers for turbulence (which one would also naively expect to be of order unity), this originates in the (still unknown) mechanism that sustains turbulence.

Equations (17) and (19) must be satisfied simultaneously, and this is possible only if Re_m depends on the relative gap width:

$$\mathrm{Re}_m \sim \frac{1}{\gamma^2}\left(\frac{\Delta r}{r}\right)^2 , \tag{20}$$

which explains the behavior seen in Figure 3. Equivalently,[10] $r^3(d\Omega/dr)/\nu \gtrsim 1/\gamma^2$; this shows that, as soon as $\Delta r \gtrsim \Delta_c$, the width of the flow does not influence the onset of turbulence, which becomes a purely local phenomenon.

The velocity fluctuation amplitude now reads

$$v_M \sim \gamma \frac{r^2\Delta\Omega}{\Delta r} \simeq \gamma r^2 \frac{d\Omega}{dr} \,, \tag{21}$$

i.e., it is proportional to the local shear rate. As a consequence, the turbulent viscosity becomes

$$\nu_t \sim \gamma^2 r^3 \frac{d\Omega}{dr} \,. \tag{22}$$

A similar relation has also been proposed by Richard & Zahn (1999) directly from experimental torque data. Note that the reasoning leading to equation (22) implicitly assumes that the flow compression plays little role, so that this result may not necessarily apply to supersonic turbulence. In order for equations (20) and (22) to faithfully account for the properties[11] of Couette-Taylor flows described in § 2.2, one needs to tie up a few loose ends:

1. Because the Coriolis force does not seem to affect the minimal Reynolds number of turbulence (see the closing comment of § 2.2), the argument above must apply to any value of $q < 2$ (the parameter introduced in § 2.3 to characterize the local rotation profile), and not only to situations with the inner cylinder at rest; however, for $q \sim 1$, the geometric term is always comparable to the advection term, and the argument is less transparent.

2. The gap relative width in Figure 3 is measured with respect to the mean radius of the rotating cylinders, whereas a local value is used above. However, the relative gap widths shown in this figure are all sufficiently smaller than unity to make the difference between the two quantities negligible in the scaling argument developed here. Incidentally, this shows again that turbulent properties are local; e.g., turbulent eddies become larger when one moves outward in a sufficiently wide cylindrical system. Correspondingly, equation (19) also follows directly from the fact that r is the only available local scale.

3. The relations derived above imply that $\gamma^2 = \beta = \mathrm{Re}^{*-1}$, but the values quoted in § 2.2 for the last two quantities differ by a factor of 6. However, it was also pointed out there that the value of $\mathrm{Re}^* \simeq 6 \times 10^5$ is overestimated, leading to a ratio ν_t/ν, which is too large because of the particular experimental protocol adopted by Taylor (1936) and Wendt (1933). Also, recent (still unpublished) experiments on Couette-Taylor flow in the "Keplerian" regime ($q = 3/2$) exhibit sustained turbulence for Reynolds numbers smaller than the limit of Figure 2, but with a different experimental protocol (Richard 2001). Therefore, it is reasonable to assume that β is a much better measure of γ^2 than Re^*; this assumption is made in the remainder of this paper, and β is used everywhere instead of γ^2.

The critical value of the relative gap width Δ_c which separates the planar regime from the rotating one obtains when the values of l_M in both regimes are equal. This yields

$$\Delta_c \equiv \left(\frac{\Delta r}{r}\right)_c \sim \left(\beta \mathrm{Re}_p\right)^{1/2} , \tag{23}$$

where $\mathrm{Re}_p \sim 2000$ is the minimal Reynolds number in the planar limit. This gives $\Delta_c \sim 1/7$, which is somewhat larger than the value of $1/20$ shown on Figure 3 (but closer to the uneducated guess $\Delta_c \sim 1$), because of the reduction adopted above in the value of Re^*.

Note also that $l_M \sim r/300$. One might wonder why such a small length scale arises, where one would naively expect $l_M \sim r$ on dimensional grounds. However, the same type of dimensional argument would also predict that turbulence sets in for $\mathrm{Re} \gtrsim 1$, which is strongly violated by the empirical evidence. The two facts have the same physical origin: the (as yet not understood) mechanism that sustains turbulence.

Two other explanations of the behavior of the Reynolds number with relative gap width have previously been proposed in the literature. Zeldovich (1981) assumed that turbulence in these Couette-Taylor flows is controlled by a competition between the epicyclic (stabilizing) frequency and the shear rate that is the source of the turbulent motions; however his findings are inconsistent with some of the data (see the discussion of this point in the appendix of Richard & Zahn 1999). Dubrulle (1993) looks for an explan-

[9] This reasoning is somewhat similar to the one which imposes that $l_M \propto y$ in the vicinity of the wall in Couette or channel flows, and which has lead to the derivation of the well-known "law of the wall," describing the mean structure of turbulent flows close to the wall (e.g., Landau & Lifshitz 1987; Tennekes & Lumley 1972; Lesieur 1987).

[10] Remember that Δr and $\Delta\Omega$ have been introduced in equations (17) and (18) to represent local gradients in order of magnitude.

[11] Most notably, the scaling of the Reynolds number with $(\Delta r/r)^2$ in the rotation regime, and the near coincidence between β and Re^{*-1}.

ation in terms of finite-amplitude instabilities in the WKB approximation, but this is incompatible with the fact that the scale r plays a key role in the problem.

I conclude this section by pointing out that the Coriolis force appears nowhere in the arguments presented in this section, which suggests that it plays little role in the development of turbulence in subcritical Couette-Taylor flows, at least for $q \sim 1$–2. Indeed, in opposition to the inertial (geometric) terms, the Coriolis force does not single out any length scale. In particular, the ratio of the advection term ($\sim w\nabla w$) to the Coriolis one ($\sim w\Omega$) in equation (8) is ~ 1 both at scale l_M and at scale Δr for the values $|q| \sim 1$–2 of interest here, and increases with decreasing scale in a Kolmogorov cascade picture. However, it does play a role in the loss of turbulence in simulated rotating flows, but this apparent paradox cannot be investigated in the framework of the order-of-magnitude arguments developed in this section. The next section is devoted to a discussion of this point.

3.4. *The Role of the Coriolis Force: Beyond Orders of Magnitude*

The question I want to address here is the following: Why is turbulence lost in numerical simulations of sheared flows when even a small amount of rotation is added (and the resulting flow remaining linearly stable)—in particular for Couette flows and disk flows in the shearing sheet approximation—whereas in experiments as different as the Couette-Taylor and rotating free shear layers, it is maintained (in the same conditions of linear stability). The forms of the Navier-Stokes equation for these flows given in § 2 strongly suggest that this is a consequence of the Coriolis force, as this is the only new force term that is taken into account when rotation is added to free shear layers and planar Couette flows in these simulations.

More specifically, clues to the role of the Coriolis force can be found by inspecting the behavior of plane Couette and free shear flows with and without rotation. The most noticeable and important feature is that, in numerical simulations of rotating Couette flows, even a small Coriolis term is able to suppress the very largest scales of the turbulent motions. This is particularly obvious, e.g., when comparing Figures 7 and 20 of Komminaho et al. (1996), which shows that the very large scales that develop in the streamwise direction in turbulent flows break up for rotation numbers as small as a few percent. This feature is quite understandable on the basis of the velocity spectra shown in Bech et al. (1995), which imply that kv_k is most likely sensibly smaller than Ω at scales larger than l_M. A similar feature can also be indirectly found in Bidokhti & Tritton (1992; see their Figs. 11 and 14, to be combined with their Fig. 16), who show that the Reynolds stress tensor magnitude decreases by a factor[12] of at least 10 when the parameter S introduced in equation (5) varies from 0 to $\lesssim -1$; this suggests that the size of the largest turbulent scales in these flows is also substantially reduced under the action of the Coriolis force.[13] This indicates that, although equation (17) always provides reliable orders of magnitude for l_M, it underestimates the relevant eddy scale by a factor of ~ 3 for nonrotating flows (see the Appendix), while overestimating it by at least the same factor once rotation is introduced. As a consequence, the loss of turbulence in the numerical simulations of rotating Couette flows of Bech & Andersson (1997) and Komminaho et al. (1996) is clearly an effect of the limited small-scale resolution due to the large box sizes (especially in the streamwise direction) adopted in these works: the smallest available scales do not allow these authors to account for the inertial part of the energy spectrum, while all the larger scales are wiped out by the Coriolis force. It is more than likely that, in these simulations, the Coriolis force kills the large-scale mechanism that has been identified to sustain turbulence in plane Couette flow simulations (Jiménez & Moin 1991; Waleffe 1997; Hamilton et al. 1995; see also § 2.1). The fact that free rotating layers and Couette-Taylor flows remain turbulent at larger levels of rotation than the ones to which turbulence is lost in these simulations implies that a different mechanism for sustaining turbulence is at work in these flows, and that it operates at scales comparable to, but apparently smaller than, the estimate of equation (17). This other mechanism has not yet been found in numerical simulations. It would be interesting to know whether this change of mechanism is related to the fact that the Coriolis force apparently selects the direction of instability of finite-amplitude defects (Johnson 1963).

The same line of argument applies to the shearing sheet simulations of Balbus et al. (1996) and Hawley et al. (1999). Indeed, the effective Reynolds number of these simulations is not an issue, since the code used by Hawley et al. (1995, 1999) is able to find turbulence (or at least the large-scale mechanism already alluded to) in nonrotating Couette flows, and this happens only for Reynolds numbers larger than at least 1500. In addition, the argument developed in § 3.2 shows that the Coriolis force by itself should not change the minimal Reynolds number for the onset of turbulence, an inference confirmed by the fact that turbulence is seen developing in the rotating free shear layer of experiments of Bidokhti & Tritton (1992) for roughly comparable Reynolds numbers. Under the assumption (cf. the arguments developed above) that equation (17) provides an estimate for the largest turbulent scale that is overestimated by a factor of at least 3 in the presence of a Coriolis force term, one obtains $l_M \lesssim \Delta y/100$, with (possibly much) smaller values more than likely. This is most probably too close to the largest resolution achieved in the shearing sheet simulations (the number of zones in any direction being no larger than 250), especially when artificial viscosity is taken into account, for turbulence to show up in these simulations.

To conclude this section, it is worth noting that some other numerical questions must be considered to find turbulence in these systems. First, it is well known from experiments with subcritical flows that the way perturbations of the flow are designed has an influence on the appearance of turbulence. This suggests that some care must be exercised in the choice of the initial conditions in numerical experiments; in particular, it might be useful to ensure that at least some condition of finite-amplitude instability is satisfied in this choice. Second, the role of the choice of the Courant number is not completely obvious, even in situations in which the CFL condition is not violated. For example, in a series of yet unpublished simulations of linearly stable

[12] The noise in the data at large rotation number does not permit a very precise estimate of this reduction factor, but the value of 10 quoted here seems a bare minimum.

[13] Note that in Bidokhti & Tritton (1992), as pointed out by the authors themselves, turbulence is not lost, and the flow remains three-dimensional, although the velocity fluctuations anisotropy is clearly affected by rotation.

Couette-Taylor flows performed with the ZEUS code in collaboration with David Clarke, we did initially find that turbulence would set in for flows that are "not too far" from planar Couette flows (including some roughly Keplerian flows), but it would eventually disappear when the maximal allowed time step was reduced, although the CFL condition was satisfied in all runs. The reason for this behavior has not yet been completely elucidated, but it appears to have some direct connection to the question of resolution just discussed.[14] In any case, the disappearance of turbulence in numerical simulations of Couette-Taylor flows that are experimentally known to be turbulent is a serious cause of worry for the reliability of the conclusions drawn from the published shearing sheet numerical experiments.

4. SUMMARY AND ASTROPHYSICAL IMPLICATIONS

Equations (17) and (18) (§ 3.2), along with their consequences, constitute the central findings of this paper. They express the natural length and velocity scales that are involved in turbulent transport in subcritical flows in terms of the local mean characteristics of the flow, and result from the constraint that the turbulent transport dominates over the viscous in the framework of the turbulent viscosity description. The scaling and orders of magnitudes implied by these relations are supported by the available experimental and numerical evidence (see the Appendix and the beginning of § 3.4).

These scaling relations have two important consequences. First, they provide an explanation for the minimum Reynolds number dependence on the relative gap width in Couette-Taylor experiments, displayed in Figure 3 (§ 3.3). A theoretical explanation of this behavior has long been sought, but none has satisfactorily been proposed yet; the phenomenological explanation presented here has the advantage of connecting apparently unrelated features, being consistent with all the experimental constraints, and pointing out the direction in which such a theoretical explanation might be looked for. Incidentally, the existence of this phenomenological explanation strengthens the validity of these scaling laws. Second, the comparison of the various flows presented in § 2 implies that disk flows described in the framework of the shearing sheet approximation should be turbulent (§ 2.4), and the scaling relations strongly suggest that the absence of turbulence in the available shearing sheet numerical simulations is due to a lack of resolution (§ 3.4). This follows because the Coriolis force destroys large-scale fluctuations, thereby affecting in a major way the nonlinear mechanism through which turbulence is maintained. At present, this mechanism is not understood, except, to some extent, for plane Couette flows.

Understanding to what extent these results are helpful in characterizing and quantifying turbulent transport in accretion disks is an important issue. Three factors at least must be accounted for: the magnitude of the disk pressure, the vertical scale height, and the presence of a magnetic field; these factors are not macroscopically independent, but relate differently to the onset of turbulence.

The disk pressure affects the problem in two a priori different ways: first, the turbulent transport picture presented in this paper requires the underlying turbulence to be subsonic (see also Huré, Richard, & Zahn 2001); second, turbulent velocity fluctuations require a force to produce them, and only the pressure force is available to this purpose in the hydrodynamical case, independently of the details of the underlying mechanism that sustains this turbulence. The first constraint is easily quantified: turbulent motions are subsonic if $v_M/c_s \lesssim 1$ (c_s is the sound speed); in accretion disks, $c_s \sim \Omega H$, and from equation (15), this implies that $H \gtrsim l_M$ (H is the disk scale height). To quantify the second constraint, note that a given fluctuating blob of size l_M undergoes a velocity change $\delta u \sim l_M(rd\Omega/dr) \sim l_M\Omega$ over a timescale $\sim v_M/l_M \sim \Omega$, because the coupling to the shear is the source of turbulent motions at the largest scales; the largest pressure variation at any scale is $\delta P/\rho \sim c_s^2$, and requiring that the resulting pressure force at scale l_M be able to account for the turbulent velocity fluctuations at this scale requires[15] again $H \gtrsim l_M$.

The turbulent scales ($\sim l_M$) are connected to the mean flow scales through the mechanism that sustains turbulence. In an accretion disk, only two such mean flow scales are available locally: H and r. The role of r has already been discussed; the role of the vertical scale height depends on the anisotropy of the mechanism that sustains turbulence. In the absence of constraint on the nature of this mechanism for rotating shear flows, I examine in turn two limiting assumptions:

1. This process is "isotropic," i.e., the scales it requires to operate are roughly identical in all directions—shearwise, streamwise, and spanwise (this is the case, for example, for the nonlinear mechanism mentioned in § 2.1 for nonrotating plane Couette flows). In this case, the elementary box in which this mechanism operates must be of size H, which implies in particular that $\Delta r \simeq H$ in all the relations used in the previous sections of this paper. If $H/r \lesssim \Delta_c$ (cf. eq. [23]), as expected in most disk models, the rotation regime of Couette-Taylor flows is irrelevant; instead, the shearing sheet approximation applies. As argued at the end of § 2.2, the Coriolis force is not expected to sensibly affect the minimal Reynolds number of turbulence, so that $\nu_t \sim (r\Delta\Omega)H/\mathrm{Re}_p \sim 10^{-3}c_sH$, and the Shakura-Sunyaev parameter $\alpha \sim 10^{-3}$. Note in this case that the constraint $H \gtrsim l_M$ is always satisfied.

2. The process is not sensitive to the vertical scale height except through the pressure requirement described above. As a consequence, as long as $H \gtrsim \beta^{1/2}r \sim 3 \times 10^{-3}r$ (which is likely to be satisfied in accretion disks), the Couette-Taylor rotation regime applies, and $\nu_t \simeq \beta r^3 d\Omega/dr \sim \beta\Omega r^2$, so that the Shakura-Sunyaev parameter $\alpha \sim \beta(r/H)^2$ lies in the range 10^{-3} to 10^{-1}. If $H \lesssim \beta^{1/2}r$, the turbulence is supersonic. Note, however, that the extra energy dissipation taking place in shocks makes a supersonic turbulence more difficult to maintain, and the disk might heat up until $H \sim l_M$ is satisfied again, or l_M might decrease, i.e., the turbulence-maintaining process might be affected and Re_m increased, or the limiting case considered here does not apply.[16] This makes the relevance of supersonic turbulence to accretion disk theory unclear.

[14] A counterintuitive dependence of hydrodynamic simulations on the Courant number is also visible on Fig. 1 of Porter & Woodward (1994).

[15] This argument ignores the possibility of supersonic turbulence.

[16] If the Reynolds number is large enough, the disk must be turbulent; this follows by considering a narrow enough disk portion so that H exceeds its width, and at least one of the regimes of the previous sections does apply, inasmuch as boundary conditions are not essential to the onset of turbulence, as argued above.

The conclusion of this brief discussion is that in the Shakura-Sunyaev parameterization of the turbulent viscosity in hydrodynamic disks, either $\alpha \sim 10^{-3}$ or $\alpha \sim 10^{-5}(r/H)^2$, depending on the unknown characteristics of the mechanism that sustains turbulence. In principle, one should also check that $\mathrm{Re} > \mathrm{Re}_m$; since $\nu \sim lc$ (where $c \sim c_s$ is the velocity dispersion and l the mean free path), this translates into $H/l \gtrsim 10^3$ in the first case above, and $r^2/Hl \gtrsim \beta^{-1} \sim 10^5$ in the second, but both requirements are most probably satisfied everywhere in astrophysical accretion disks.

It is unclear how the presence of a magnetic field can modify hydrodynamic shear turbulence. In particular, even a dynamically nondominant field can easily affect the mechanism of generation of turbulence, and therefore significantly modify the efficiency of the turbulent viscosity transport, on top of adding a turbulent resistivity, even if the MHD flow remains linearly stable.[17]

[17] This can happen, e.g., if the disk scale height is small enough as to not let any magnetorotational mode become unstable, which is easily realized in disks with a near equipartition between thermal and magnetic energies.

Conversely, the possible occurrence of hydrodynamic shear turbulence might possibly affect in a major way our present understanding of MHD transport and dynamo processes in accretion disks, which mostly relies on the physics of the nonlinear development of the magnetorotational instability. Clarifying these questions is of primary importance for accretion disk theory.

To conclude this paper, let me point out that there is one example of a Keplerian disk that has been observed with a great luxury of details, and that is not turbulent, namely, Saturn's rings. However, the requirements discussed above fail on several accounts in ring systems, because both the particle size d and mean free path l are comparable to H. For example, in the first limiting case discussed above, the ring is necessarily laminar, while in the second, because $H \gtrsim l_M$, the granularity of the system makes scales $\lesssim l_M$ inaccessible to the fluid description; the same argument makes supersonic turbulence most probably irrelevant to ring systems.

APPENDIX

EVIDENCE FOR THE PROPOSED TURBULENT SCALING

Because Re_m is at least of the order of 10^3, the order-of-magnitude estimates of equations (17) and (18) are sensibly smaller than the mean flow length and velocity scales to which l_M and v_M are usually assumed to be comparable. Nevertheless, they are in good order-of-magnitude agreement with the available evidence. Consider, for example, the simulation of Couette flow reported in Bech et al. (1995), and further exploited in Bech & Andersson (1996b) to quantify the structure of the Reynolds stress in the central region of Couette flows. For Couette flows, equation (18) gives $v_M \sim \Delta v_x/40$. The simulation just mentioned has a Reynolds number[18] of 5200, i.e., well above the threshold of transition to turbulence. The behavior of the Reynolds stress as a function of the distance to the wall is represented on Figure 1*a* of Bech & Andersson (1996b), and, after accounting for the particular normalization adopted in their graph,[19] one finds $v_M \simeq \Delta v_x/30$ for this simulation, which is nearly identical to the estimate deduced from equation (18). Even if one takes into account the fact that the value of Δv_x relevant for the bulk of the flow is smaller than the one adopted in equation (18) by a factor of $\sim$4, the two estimates of v_M still agree within a factor of $\sim$3. Another estimate of the same quantity for nonrotating free shear flows is obtained from the representation[20] of $\langle \delta v_x \delta v_y \rangle$ in Figure 14 (at $Q = 0$) of Bidokhti & Tritton (1992), and gives $v_M \sim \Delta v_x/10$, which differs from the order-of-magnitude estimate quoted above by a factor of $\sim$4. Some indication of the value of l_M can also be extracted from Figure 2 of Bech et al. (1995), which shows the power spectra in the shearwise and spanwise directions. However, the box size in these directions is large in terms of h, and the resolution of the simulation does not allow the authors to really reach the inertial part of the turbulent spectrum. This is particularly noticeable for k_x spectra in the middle of the flow (displayed in the $y = 82$ quadrant of this figure), which are nearly flat down to $k_x h \simeq 10$, and drop precipitously for larger values of k because of numerical dissipation, as the limit resolution of the simulation is reached. The k_z spectra behave sensibly better, most probably because the box is 2.5 times smaller in this direction, and show some indications that an inertial spectrum tries to develop for $8 \lesssim k_z h \lesssim 30$. Because $h = \Delta y/2$, this suggests that l_M in this simulation is at most within a factor of $\sim$3 of the order-of-magnitude estimate deduced from equation (17). Note in passing that, for Couette flows, the inertial spectrum does not need to be resolved in order for turbulence to be observed in numerical simulations; this is related to the existence of a large-scale nonlinear mechanism that sustains turbulence, as mentioned in § 2.1, and which is most likely at the origin of the more or less flat part of the spectra at large scales.

[18] Note that our definition of the Reynolds number differs from the one adopted in these papers by a factor of 4.

[19] A property of Couette flows is that the total mean shear stress $\tau = \rho(\nu d\langle v_x \rangle/dy - \langle \delta v_x \delta v_y \rangle)$ is constant in the shearwise direction (this follows from the stationarity of the mean flow). Away from the wall $\tau \simeq -\rho\langle \delta v_x \delta v_y \rangle$, whereas close to the wall $\tau \simeq \rho\nu d\langle v_x \rangle/dy$; consequently, the Reynolds stress is usually normalized to τ/ρ, velocities to $v_\tau \equiv (\tau/\rho)^{1/2}$, and one has $v_M \simeq v_\tau$ in the bulk of the flow. The value of v_τ for this simulation can be obtained in the following way. Note first that Figure 1*a* of their paper also displays $\mathrm{Re}_\tau^{-1} d\langle v_x \rangle/dy$ where, for their simulation, $\mathrm{Re}_\tau = v_\tau h/\nu = 82$, and where v_x is normalized to v_τ and y to the walls half-distance h; this quantity is equal to 1 in the immediate vicinity of the wall. On the other hand, the value of the velocity gradient near the wall in units of $2U_w/h = \Delta v_x/h$ can be deduced from Figure 4 of Bech et al. (1995), which relates to the same simulation. The comparison of these two measures of the same quantity yields the required value of $v_\tau/2U_w$.

[20] Note that v_M characterizes turbulent transport, and that $\langle \delta v_x \delta v_y \rangle$ is usually smaller than the magnitude of velocity fluctuations by a factor of a few.

REFERENCES

Andereck, C. D., Liu, S. S., & Swinney, H. L. 1986, J. Fluid Mech., 164, 155
Balbus, S. A., & Hawley, J. F. 1991, ApJ, 376, 214
Balbus, S. A., Hawley, J. F., & Stone, J. M. 1996, ApJ, 467, 76
Bech, K. H., & Andersson, H. I. 1996a, J. Fluid Mech., 317, 195
———. 1996b, Fluid Dyn. Res., 18, 65
———. 1997, J. Fluid Mech., 347, 289
Bech, K. H., Tillmark, N., Alfredsson, P. H., & Andersson, H. I. 1995, J. Fluid Mech., 286, 291
Bidokhti, A. A., & Tritton, D. J. 1992, J. Fluid Mech., 241, 469
Brandenburg, A., Nordlung, A., Stein, R. F., & Torkelsson, U. 1995, ApJ, 446, 741
Casse, F., & Ferreira, J. 2000, A&A, 353, 1115
Chandrasekhar, S. 1960, Proc. Natl. Acad. Sci., 46, 53
Dauchot, O., & Daviaud, F. 1994, Phys. Fluids, 7, 335
Dubrulle, B. 1993, Icarus, 106, 59
Dubrulle, B., & Zahn, J.-P. 1991, J. Fluid Mech., 231, 561
Ferreira, J. 1997, A&A, 319, 340
Fleming, T. P., Stone, J. M., & Hawley, J. F. 2000, ApJ, 530, 464
Hamilton, J. H., Kim, J., & Waleffe, F. 1995, J. Fluid Mech., 287, 317
Hawley, J. F., Balbus, S. A., & Stone, J. M. 2001, ApJ, 554, L49
Hawley, J. F., Balbus, S. A., & Winters, W. F. 1999, ApJ, 518, 394
Hawley, J. F., Gammie, C. F., & Balbus, S. A. 1995, ApJ, 440, 742
Huré, J.-M., Richard, D., & Zahn, J.-P. 2001, A&A, 367, 1087
Jiménez, J., & Moin P. 1991, J. Fluid Mech., 225, 213
Johnson, J. A. 1963, J. Fluid Mech., 17, 337
Komminaho, J., Lundbladh, A., & Johansson, A. V. 1996, J. Fluid Mech., 320, 259
Landau, L. D., & Lifshitz, E. M. 1987, Fluid Mechanics (2d Ed.; Oxford: Pergamon)
Lerner, J., & Knobloch, E. 1988, J. Fluid Mech., 189, 117
Lesieur, M. 1987, Turbulence in Fluids (Dordrecht: Kluwer)
Marcus, P. S. 1984a, J. Fluid Mech., 146, 45
———. 1984b, J. Fluid Mech., 146, 65
Porter, D. H., & Woodward, P. R. 1994, ApJS, 93, 309
Prandtl, Z. A. 1925, Zs. Angew. Math. Mech., 5, 136
Richard, D. 2001, Ph.D. thesis, Univ. Paris VII
Richard, D., & Zahn, J.-P. 1999, A&A, 347, 734
Sano, T., Miyama, S. M., Umebayashi, T., & Nakano, T. 2000, ApJ, 543, 486
Taylor, G. I. 1936, Proc. R. Soc. London A, 223, 289
Tennekes, H., & Lumley, J. L. 1972, A First Course in Turbulence (Cambridge: MIT Press)
Terquem, C. 2001, preprint (astroph/0107408)
Tillmark, N., & Alfredsson, P. H. 1992, J. Fluid Mech., 235, 89
Tritton, D. J. 1992, J. Fluid Mech., 241, 503
Waleffe, F. 1997, Phys. Fluids, 9, 883
Wendt, F. 1933, Ing. Arch., 4, 577
Zeldovich, Y. B. 1981, Proc. R. Soc. London A, 374, 299